AIAA SciTech Forum
7-11 January 2019, San Diego, California
AIAA Scitech 2019 Forum

10.2514/6.2019-1648

Dynamic SGS modeling in LES using DG with kinetic energy preserving flux schemes

Michael Stoellinger* , Andrew Kirby † , Anthony Edmonds ‡ , Dimitri J. Mavriplis §
Mechanical Engineering Department, University of Wyoming, 1000 E. Univ. Ave., Laramie, WY 82071, USA.
and Stefan Heinz¶
Department of Mathematics, University of Wyoming, 1000 E. Univ. Ave., Laramie, WY 82071, USA

The Discontinuous Galerkin (DG) method provides numerical solutions of the Navier-Stokes equations with high order of accuracy in complex geometries and allows for highly efficient parallelization algorithms. These attributes make the DG method attractive for large eddy simulation (LES). Recently developed kinetic energy preserving flux schemes are adopted to achieve a minimally dissipative DG solver which is augmented with two different subgrid scale closure models: constant coefficient Smagorinsky Model (CCSM), and Dynamic Heinz Model (DHM). For the dynamic models, a modal cut-off filter is adopted as the test filter. We consider the Taylor-Green Vortex flow at Reynolds number Re = 1600. We find that the kinetic energy preserving flux schemes provide stable solutions for the severely under-resolved simulations using high polynomial orders at much lower cost than polynomial de-aliasing. However, it is also found that although the PI scheme very closely conserves kinetic energy in the inviscid limit, it displays significant numerical dissipation for the Re=1600 case. The constant Smagorinsky SGS model adds too much dissipation causing a too fast decay of kinetic energy. The DHM does add significantly less dissipation leading to better results than CCSM but overall a too rapid energy decay is predicted.

I. Introduction

Direct Numerical Simulations (DNS) resolves all velocity, length, and time scales in a turbulent flow and are thus computationally too expensive for all but simple problems at low Reynolds numbers. In Large Eddy Simulation (LES), only the large scales of turbulence are resolved and the small scales are modeled. Both DNS and LES require many degrees of freedom and high order methods provide accurate solutions with relatively fewer degrees of freedom compared to low order methods. Spectral methods are commonly used in DNS simulations but they are limited to periodic Cartesian grid problems. Therefore, they are too restricting since most problems of technical interest require an unstructured mesh (e.g. flow over airfoils). The Finite element method is a high order method that can handle unstructured meshes, this allows for high order accuracy within complex geometries. The particular Finite Element method used

*Associate Professor, AIAA Member, Department of Mechanical Engineering.
†Post Doctoral Research Associate, AIAA Member, Department of Mechanical Engineering
‡Graduate Student, AIAA Member, Department of Mechanical Engineering
§Professor, AIAA Fellow, Professor, Department of Mechanical Engineering
¶Professor, AIAA member, Department of Mathematics.

in this work is a Discontinuous Galerkin (DG) method. DG is used to discretize the compressible LES Navier-Stokes equations. The LES equations are obtained by applying a spatial filter (or a spectral low-pass filter) to the Navier-Stokes equations such that the small scales of turbulent motion are filtered out and the effect of these so called subgrid scales (SGS) are modeled by an additional subgrid scale viscosity. This means that by definition LES is an under-resolved simulation. For spectral methods it is well known that the effect of aliasing[1] in the non-linear convective term can cause numerical instabilities through an accumulation of energy at the high modes. In this work we will first investigate the feasibility of two different de-alisaing strategies to stabilize the numerical solution in LES without SGS model (implicit LES): polynomial de-aliasing using a sharp cut-off filter in modal space and a new approach based on kinetic energy conserving split-form flux approximations.[2,3] We also investigate the performance of two SGS models: the Smagorinsky model[4] (constant coefficient and dynamic) and a dynamic model developed by Heinz.[5] The constant coefficient Smagorinsky model (CCSM) requires the specification of the model coefficient C_s and the scalar filter scale Δ of the low-pass filter operation that is used to derive the LES equations. With most low order LES investigations using finite volume or finite difference methods, the low-pass filter operation is not explicitly performed. Instead, it is assumed that the numerical discretization of the derivatives acts as filter similar to a top-hat filter in space with a filter scale Δ that is equal to the grid spacing δ_x. For the finite volume method the definition is usually given by[4] $\Delta = V_c^{1/3}$ where V_c is the cell volume. In high order DG methods, using the cubic root definition is not appropriate since each DG element approximates the solution to a high order and hence it is not clear what expression should be used to obtain Δ from the element size and polynomial order. A second problem with the CCSM model is that the model coefficient C_s is flow dependent and hence different values are required for different flows. More over, the CCSM model does not perform well in flows that transition from the laminar to the turbulent state. For such flows, the CCSM model predicts a SGS viscosity in all flows with velocity gradients and this added SGS viscosity usually delays the laminar - turbulent transition significantly. Dynamic SGS models such as the dynamic Smagorinsky model or the dynamic model developed by Heinz[5] (DHM) calculate the model coefficient dynamically based on the flow state. The dynamic models require the explicit application of a so called test filter operation that is used to determine the model coefficient locally based on turbulence scaling laws. The DHM dynamic model[5] is derived from an underlying stochastic turbulence model leading to improved predictions compared to the DSM for certain flows.[5] In theory, the dynamic models should be able to predict laminar - turbulent transition if the dynamic procedure in a laminar flow results in $C_s = 0$ and hence a negligible SGS viscosity. We will investigate the suitability of using the sharp cut-off filter in modal space as a test filter for the dynamic models and evaluate their model performance compared to the CCSM. The flow under consideration is the Taylor Green Vortex test case[6] at a Reynolds number of $Re = 1600$. At this Reynolds numbers, the flow transitions from an initially laminar vortical flow (prescribed by an analytical velocity field) to a turbulent flow not dissimilar to freely decaying grid generated turbulence. The flow is thus very challenging for any SGS model.

II. Numerical Formulation

A. Discontinuous Galerkin Solver

The governing equations are the compressible Navier- Stokes equations representing the conservation of mass, momentum, and energy and are given by:

$$\frac{\partial}{\partial t}\begin{bmatrix}\rho\\ \rho u\\ \rho v\\ \rho w\\ \rho E\end{bmatrix} + \frac{\partial}{\partial x}\begin{bmatrix}\rho u\\ \rho u^2 + p - \tau_{11}\\ \rho uv - \tau_{21}\\ \rho uw - \tau_{31}\\ \rho uH - \tau_{1i}u_i + q_1\end{bmatrix} + \frac{\partial}{\partial y}\begin{bmatrix}\rho v\\ \rho uv - \tau_{12}\\ \rho v^2 + p - \tau_{22}\\ \rho vw - \tau_{32}\\ \rho vH - \tau_{2i}u_i + q_2\end{bmatrix} + \frac{\partial}{\partial z}\begin{bmatrix}\rho w\\ \rho uw - \tau_{13}\\ \rho vw - \tau_{23}\\ \rho w^2 + p - \tau_{33}\\ \rho wH - \tau_{3i}u_i + q_3\end{bmatrix} = 0,$$

where ρ is the density, u, v, w are the velocity components in each spatial coordinate direction, p is the pressure, E is total internal energy, $H = E + p/\rho$ is the total enthalpy, τ is the viscous stress tensor, and

q is the heat flux. The viscosity is a function of the temperature given by the Sutherland's formula. These equations are closed using the ideal gas equation of state:

$$\rho E = \frac{p}{\gamma - 1} + \frac{1}{2}\rho(u^2 + v^2 + w^2)$$

where $\gamma = 1.4$ is the ratio of specific heats. In all of the following, Einstein notation is used where the subscript i represent spatial dimensions and has a range of 1 to 3. The solution vector is comprised of the conservative variables and is shown under the time derivative.[7]

Discontinuous Galerkin (DG) methods combine ideas of finite element and finite volume methods allowing for high-order approximations and geometric flexibility. The solver utilizes the Lax-Friedrichs[8] method and kinetic energy conserving schemes[2,3] for the inviscid flux routine and a symmetric interior penalty (SIP)[9,10] viscous flux routine. The governing equations are marched in time using an explicit 4-stage (fourth order) Runge Kutta method.[11] If used as an LES solver with an SGS model the SGS viscosity is simply added to the molecular viscosity and the viscous flux contains both molecular and turbulence contributions. The intent of this code is to be used as a far body solver with over-set capabilities and it is designed for high speed performance and robustness capable of only structured Hexahedron meshes. DG is a subset of the Finite-Element Method where each element is projected from physical space to a reference space. A polynomial basis is used to approximate the solution in the projected reference space. All basis are equivalent however it is often advantageous to pick a basis for certain characteristics. The basis used for this solver is the Lagrange Nodal basis evaluated at Gauss Lobatto Quadrature points[12] and the number of Gauss quadrature points ngp is related to the polynomial degree of approximation by $ngp = P + 1$. The basis and test function are created using a tensor product of Lagrange Interpolating polynomials which is a non-hierarchical nodal basis. Polynomial orders of $P = 1$ up to $P = 15$ are considered in this work. A great advantage of the DG method over continuous Spectral Elements is the high parallel efficiency capability, allowing for greatly reduced simulation run times.

B. Filter Implementation in DG

Within the framework of a DG solver, high frequency content of the solution is stored in the higher order modes of the polynomial basis. The Nodal basis used in this solver is not hierarchical, i.e. each mode of the basis contains high order content[13] as can be seen in Figure 1A which shows the basis functions of the nodal basis for $ngp = 4$ (highest polynomial degree $P = 3$). In a hierarchical basis such as the Legendre Modal basis, only the higher order modes contain higher order polynomial degrees as can be seen from Figure 1 B. Filtering in a hierarchical basis is straight forward since specific higher order modes can be damped by multiplying the corresponding solution coefficient with value between 0 and 1. If certain higher order modes are completely removed and the lower order modes are not affected then one speaks of a sharp modal cut-off filter. Such filters have the nice property that a repeated application of the filter has the same outcome as a single application of the filter. Higher order modes can not directly be removed from a "nodal" basis. By transforming the solution given in a "nodal" basis to a solution given in a "modal" basis the coefficients of the higher order modes can be modified and then the modified coefficients in the "modal" basis are transformed back into the "nodal" basis.[13–15]

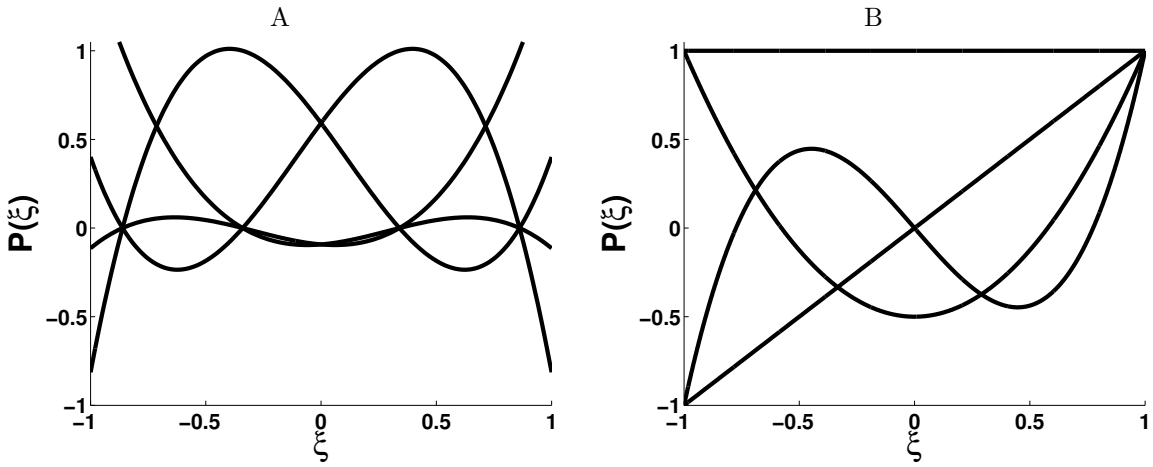

Figure 1. Basis functions up to polynomial degree $P = 3$ for A: the Nodal basis (Gauss-Lobatto Lagrange polynomials) with $ngp = 4$ and B: the Legendre Modal Basis

Here we follow the procedure outlined by Gassner et al.[14] The "nodal" mass matrix $\mathbf{M}$ and solution coefficients b and mixed "modal" mass matrix $\mathbf{C}$ and solution coefficients a are related by

$$U = \mathbf{M}b = \mathbf{C}a,$$

where U denotes the approximation of the solution. We denote the Nodal Basis by $\psi(\xi_i)$, the Modal Basis by $\phi(\xi_i)$, ξ are the Gauss-Lobatto Quadrature Points, and w_k are the Gauss-Lobatto weights associated with each quadrature point. The mass matrices are defined by

$$M_{ij} = \int_{-1}^{1} \psi\psi^T d\Omega = \sum_{k=1}^{ngp} \psi_i(\xi_k)\psi_j(\xi_k)w_k, \tag{1}$$

$$C_{ij} = \int_{-1}^{1} \psi\phi^T d\Omega = \sum_{k=1}^{ngp} \psi_i(\xi_k)\phi_j(\xi_k)w_k. \tag{2}$$

The solution coefficients in the modal basis b are obtained by

$$b = \mathbf{M}^{-1}\mathbf{C}a. \tag{3}$$

Once the coefficients in the Modal Basis b are obtained, the filter operation is simply a matrix vector multiplication

$$\widehat{b} = \mathbf{F}b, \tag{4}$$

where $\mathbf{F}$ is the sparse filter matrix (for the modal basis) and the hat symbol indicates that the coefficients have been filtered. For the sharp modal cut-off filter, the value of $F_{i,i}$ where i is the particular mode to be modified is set to one for all $i \leq P_c$ and is set to zero for all $i > P_c$ where P_c is the desired cut-off mode. By using

$$a = \mathbf{C}^{-1}\mathbf{M}b, \tag{5}$$

and substituting the modal coefficients b with filtered modal coefficients $\widehat{b}$ gives the filtered solution coefficients $\widehat{a}$ in the nodal basis

$$\widehat{a} = \mathbf{C}^{-1}\mathbf{M}\left(\mathbf{F}b\right). \tag{6}$$

By introducing the matrices

$$\mathbf{B} = \mathbf{C}^{-1}\mathbf{M}, \;\; \mathbf{B}^{-1} = \mathbf{M}^{-1}\mathbf{C}, \tag{7}$$

and

$$\widehat{F} = \mathbf{B}^{-1}\mathbf{F}\mathbf{B}, \tag{8}$$

we can finally write the sharp modal cut-off filter operation as

$$\widehat{a} = \widehat{\mathbf{F}} a. \tag{9}$$

It is worth noting that the modified filter matrix $\widehat{\mathbf{F}}$ can be assembled as a pre-processing step and does not have to be recalculated during the simulation. Fig. 2 shows a simple 1-D example of the modal filtering approach. We use a function f that has a low and high frequency content $f(x) = cos(2.*x) + 0.3*sin(8*x)$ (black line) on the interval $[-\pi, \pi]$. The function is well approximated by DG (green line) on $N = 6$ elements with a polynomial degree $P = 4$ (hence using $ngp = 5$ quadrature points shown as green dots). The discontinuous nature of the approximation is also clearly visible by the "jumps" of the approximation at the element boundaries. Applying the sharp modal cut-off filter so that modes with polynomial degree larger than one are removed ($P_c = 1$) leads to the piece-wise linear approximation indicated by the red line in fig. 2. Clearly, the sharp modal cut-off filter is able to remove the high frequency content of the function f.

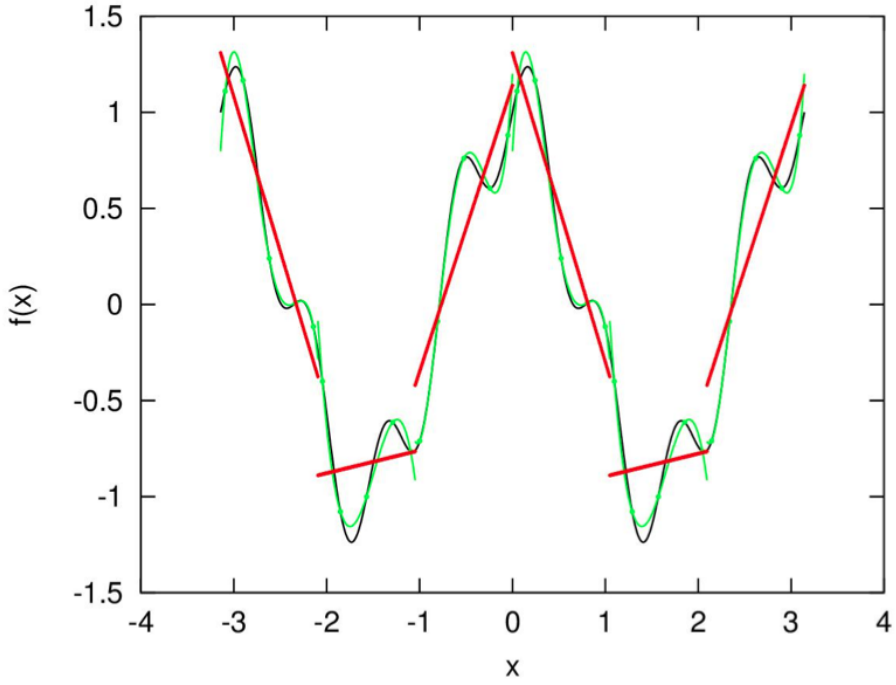

Figure 2. One dimensional example of the sharp spectral cut-off filter. Original function $f(x) = cos(2.*x) + 0.3*sin(8*x)$ (black line), DG approximation on $N = 6$ elements with fourth order polynomials $P = 4$ (green line, dots represent the $ngp = 5$ quadrature points on each element), and filtered solution using the sharp spectral cut-off filter with $P_c = 1$ (red line).

C. Polynomial dealiasing using a sharp modal cut-off filter

Polynomial aliasing occurs in under resolved simulations due to the quadrature errors that are introduced when calculating inner products of the non-linear convective terms in the Navier-Stokes Equations.[1] The errors can lead to a build up of energy in the higher order modes and hence lead to instabilities of the simulations. For DG simulations with lower polynomial orders there seems to be sufficient numerical dissipation such that the energy in the higher order modes is dissipated sufficiently fast.[14,15] For higher polynomial approximations which are more desirable from a convergence point of view and also for better parallel efficiency the numerical dissipation is greatly reduced and not sufficient to remove the aliasing errors. One method to prevent polynomial aliasing is to use more quadrature points in the evaluation of the inner products of

the non-linear terms. However, this would require a significant alteration of the DG code. A second more straight forward method is to increase the number of solution quadrature points for all solution operations by increasing P (P+1 quadrature points) and then projecting the solution back to a lower order P_c by applying the sharp modal cut-off filter. We will apply this method for polynomial de-aliasing to test the implementation of the modal cut-off filter (which will later also be used for the dynamic SGS models). This polynomial de-aliasing approach has previously been adopted by Laslo et al[15] and Gassner et al.[14] In the context of LES, polynomial de-aliasing can be viewed as an explicitly filtered LES.

III. LES SGS Models considered

A. Smagorinsky Model

The LES equations are obtained by applying a low-pass filter to the Navier-Stokes equations such that the small scales of turbulent motion are filtered out and the effect of these so called subgrid scales on the resolved scales are most commonly modeled by an additional subgrid scale viscosity. The SGS viscosity provides the additional dissipation that occurs in the unresolved small scales. We will denote the low pass-filter operation used to derive the LES equations by an overbar e.g. $\overline{\rho}$ denotes the filtered density. In compressible flows, turbulence modeling is based on density weighted (Favre) filtering[4] for all variables except pressure and density. For example, the Favre filtered velocity is

$$\widetilde{u} = \frac{\overline{\rho u}}{\overline{\rho}}. \tag{10}$$

As mentioned in the introduction, in most LES applications the low-pass filter operation (called the grid filter) is not performed explicitly, but implicitly through the numerical approximation. In this work, we consider cases without using an explicit low-pass filter operation and cases where we us the sharp modal cut-off filter as grid filter. The additional SGS viscosity is defined as

$$\mu_{sgs} = \overline{\rho}(C_s\Delta)^2 \left|\widetilde{S}\right|, \tag{11}$$

where C_s is a model parameter, Δ is the length scale associated with the grid filter and $\widetilde{S}$ is the magnitude of the Favre averaged rate of strain tensor given by

$$\widetilde{S}_{ij} = \frac{1}{2}\left(\frac{\partial \widetilde{u_i}}{\partial x_j} + \frac{\partial \widetilde{u_j}}{\partial x_i}\right), \ \left|\widetilde{S}\right| = \sqrt{2\widetilde{S}_{ij}\widetilde{S}_{ij}}. \tag{12}$$

In the constant coefficient Smagorinsky Model (CCSM) the model parameter is set to $C_s = 0.17$.[16] The commonly used definition of the filter size has to be modified in the high-order DG method considered in this work . Since the DG elements are typically much larger than finite volume cells and resolve much more detail, the filter width Δ should be defined as a function of the polynomial order of accuracy P. Here we propose the simple approach

$$\Delta = C_p \times (\Delta_x\Delta_y\Delta_z)^{1/3}, \tag{13}$$

where the parameter C_p is estimated to be given by

$$C_p = \frac{1}{2}\frac{1}{P+1}, \tag{14}$$

with P the polynomial order of approximation of the DG elements.

B. Dynamic Heinz Model Definition

In the dynamic Heinz model[5] (DHM) the Smagorinsky coefficient is calculated based on the local instantaneous flow state and hence $C_s = f(x, y, z, t)$, a function of space and time rather than simply defined as a

constant. The dynamic calculation of the coefficient is based on an explicitly performed second level filter operation called the test filter that is applied to the grid filtered variables. We denote the test filter operation by a hat e.g. the test filtered density is denoted by $\widehat{\overline{\rho}}$. Here we always use the sharp modal cut-off filter as the test filter as described in section B. The main difference to the dynamic Smagorinsky model is that now the Leonard stress tensor is modeled.

$$L_{ij} = \widehat{\overline{\rho}\widetilde{u}_i\widetilde{u}_j} - \frac{\widehat{\overline{\rho}\widetilde{u}_i}\widehat{\overline{\rho}\widetilde{u}_j}}{\widehat{\overline{\rho}}},\ L^d_{ij} = L_{ij} - \frac{1}{3}L_{kk}\delta_{ij}, \tag{15}$$

Details of the model derivation can be found in Gopalan and Heinz.[5] The model coefficient in the Heinz model is determined by

$$(C_s\overline{\Delta})^2 = -\frac{L_{ij}\widehat{\widetilde{S}_{ij}}^d}{\alpha\left|\widehat{\widetilde{S}}^d\right|^3}$$

α denotes the square of the test filter to grid filter width ratio $\alpha = (\frac{\widehat{\overline{\Delta}}}{\overline{\Delta}})^2$. Typically, $\alpha = 4$ since the test filter is often assumed to be twice the width of the grid filter.[16] In the DG method adopted in this work we calculate α using the expression for C_P (14) giving

$$\alpha = \left(\frac{(P_{grid}+1)}{(P_{test}+1)}\right)^2. \tag{16}$$

Here, P_{grid} refers to the polynomial order of the DG method if no explicit grid filter operation is used or to the polynomial order after the explicit grid filter (sharp modal cut-off with $P_{grid} = P_c$ is applied) and P_{test} is the polynomial order after applying the explicit test filter with $P_{test} < P_{grid}$. The implementation of this model in typical finite difference and finite volume solvers has shown improved results achieved with less stringent clipping or averaging of $(C_s\overline{\Delta})^2$ as compared to the DHM. Here, we clip the dynamic constant to be in the range $0 \leq C_s \geq 0.5$.

IV. Taylor Green (TG) Vortex Flow

The advantage of using the Taylor Green Vortex case is that this flow has the same initialization for every simulation and it is well documented providing a reliable comparison with other codes including DG. The Taylor Green vortex is initially laminar and becomes fully turbulent in later stages making it a challenging test case for dynamic SGS models. A disadvantage is the additional run time to obtain a fully turbulent solution. We will focus on the $Re = 1600$ case for which highly accurate DNS results[6] (obtained with a spectral code using 512 modes) are available for comparison to our DNS (for code validation) and LES model evaluation. Figure 3 shows vorticity contours at the initial condition (left) and towards the end of the run for the spectral DNS.[6]

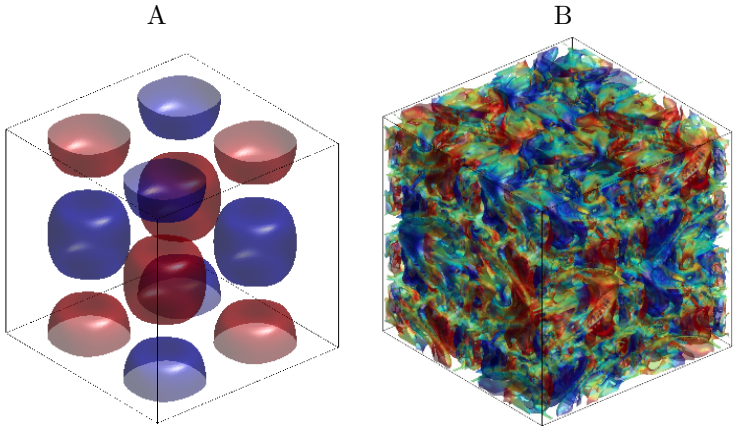

Figure 3. Taylor Green Vortex with Re=1600 showing contours of Z-Vorticity[6] at t=0 (A) and t=20 (B)

The computational domain is given by $\Omega = [-\pi L, \pi L] \times [-\pi L, \pi L] \times [-\pi L, \pi L]$ and periodic boundary conditions are applied in all directions. The Taylor Green Vortex Case was initialized based on the parameters: $L = 1$, $Re = 1600$, $U_0 = 0.1$, $\rho = 1$, $\mu = 6.25 \times 10^{-5}$, $Pr = 0.71$, and $P_0 = 0.714$. These parameters correspond to $Ma = 0.1$ such that the results can be safely compared to the incompressible spectral DNS results.[6] The initial velocity and pressure fields are given by

$$\begin{aligned} u &= U_0 sin(\frac{x}{L}) cos(\frac{y}{L}) cos(\frac{z}{L}), \\ v &= -U_0 cos(\frac{x}{L}) sin(\frac{y}{L}) cos(\frac{z}{L}), \\ w &= 0, \\ p &= p_0 + \frac{\rho_0 V_0^2}{16} \left(cos\left(\frac{2x}{L}\right) + cos\left(\frac{2y}{L}\right) \right) \left(cos\left(\frac{2z}{L}\right) + 2 \right). \end{aligned} \tag{17}$$

Relevant post processing quantities are the total kinetic energy

$$K(t) = \frac{1}{\rho_0 \Omega} \int_\Omega \rho \frac{U_i U_i}{2} d\Omega, \tag{18}$$

and the total kinetic energy dissipation rate,

$$\varepsilon(t) = -\frac{dK}{dt}. \tag{19}$$

It should be noted here that the total dissipation of kinetic energy is calculated from the kinetic energy by using a simple central difference approximation of the time derivative. Thus, the dissipation rate ε also contains contributions from the numerical dissipation.[6] Both the dissipation rate and time are normalized for comparison with results from the High Order Workshop.[6] Dissipation is normalized with $\frac{U_0^3}{L}$ and time is normalized with $\frac{L}{U_0}$. To distinguish between the total dissipation rate (including numerical dissipation) and the actually resolved dissipation rate we also consider the resolved visous dissipation

$$\varepsilon_1(t) = \frac{1}{\rho_0 \Omega} \int_\Omega 2\mu S_{ij} S_{ij} d\Omega, \tag{20}$$

and the pressure work

$$\varepsilon_3(t) = \frac{1}{\rho_0 \Omega} \int_\Omega p \cdot \frac{\partial U_i}{\partial x_i} d\Omega, \tag{21}$$

which is expected to be small in this nearly incompressible flow.

V. Results

A. Well-resolved simulations

We consider the TG vortex case at $Re = 1600$ with a resolution of $P = 6$, $N = 36$ leading to $DOF = 252^3$ for code validation. This resolution has been shown[17] sufficient to achieve good agreement with the spectral DNS results ($DOF = 512^3$) when using the DG solver with the Lax-Friedrichs flux (DGLF). Figure 4 shows a comparison between the DGLF results and the Pirozzoli Split Form (PI) for the kinetic energy (A) and kinetic energy decay rate (B). Both results are very close to each other and agree well with the DNS. Figure

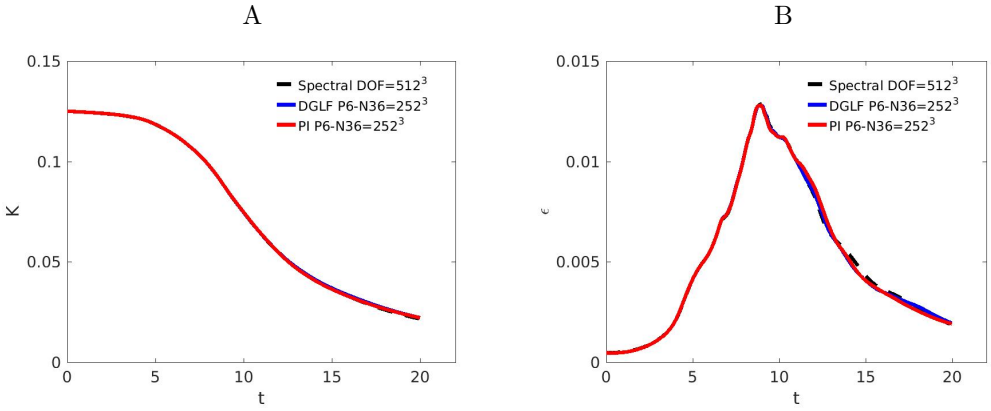

Figure 4. Kinetic energy (A) and its decay rate (B) in the Taylor Green Vortex with Re=1600 using the DGLF and PI methods with $DOF = 252^3$.

5 shows the result for the pressure work over the course of the simulation and the values stay about one order of magnitude below the total dissipation rate. To demonstrate that most of the dissipation is already

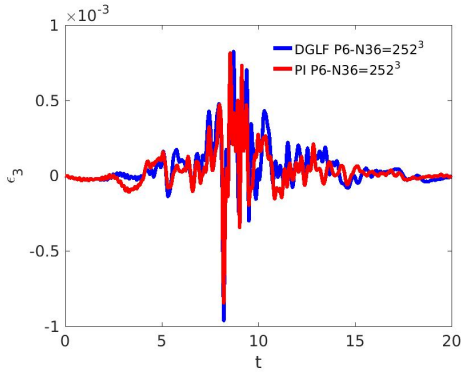

Figure 5. Pressure work for the Taylor Green Vortex with Re=1600 using the DGLF and PI methods with $DOF = 252^3$.

resolved at this resolution we compare the total dissipation ε and the resolved viscous dissipation rate ε_1 for the two approaches in figure 6. For both methods the resolved viscous dissipation is almost identical to the total dissipation rate thus indicating negligible numerical dissipation. However, it is somewhat surprising to see that the kinetic energy preserving PI method (shown in B) shows a slightly larger numerical dissipation (smaller resolved viscous dissipation) that the DG method with the dissipative Lax-Friedrichs flux.

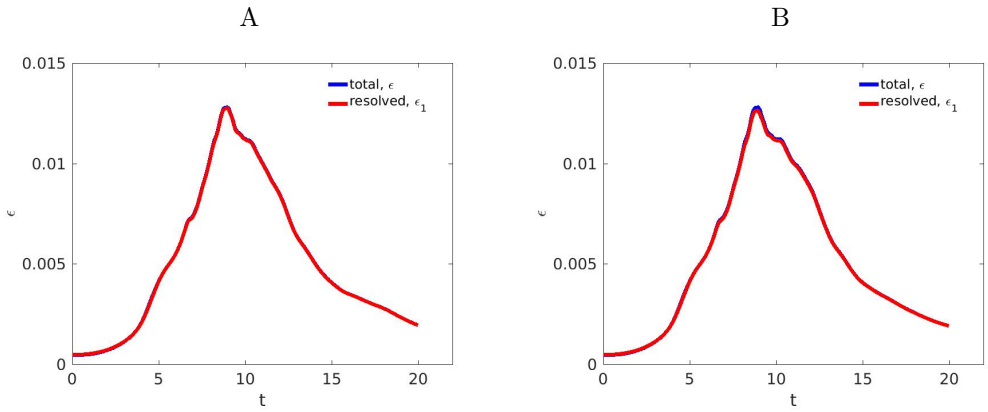

Figure 6. Comparison of the total dissipation ε and the resolved viscous dissipation rate ε_1 for the DGLF (A) and PI (B) approaches.

B. Under-resolved simulations without SGS model

We consider the TG vortex case at $Re = 1600$ with a much lower resolution of $DOF = 64^3$ compared to the quasi DNS results obtained with $DOF = 252^3$ presented in the previous section. Hence the simulations presented here can be viewed as a typical implicit LES if the dissipative DGLF is considered. It has been shown previously by several authors[14,15,17] that under-resolved DG simulations of the TG flow become numerically unstable for high orders due to polynomial aliasing. This is shown in figure 7-A where results using DGLF are shown for varying polynomial orders keeping the total DOF's constant. It can be seen that the lower order $P = 1$ and $P = 3$ simulations run stable (but are not accurate) and the high order $P = 7$ simulation becomes unstable. Using polynomial filtering with a sharp modal cut-off filter of order P_C chosen such that twice as many quadrature points are used[15] (following the $2N$ rule for de-aliasing for compressible flows) prevents the instability. This is demonstrated in figure 7-B where the modal cut-off filter is applied to the residual at every Runge-Kutta stage. Hardly any difference can be seen for the $P = 1$ and $P = 3$ case due to the dominance of the numerical dissipation. For the $P = 7$ case the effect of the de-aliasing is significant since the simulation now runs stable and provides results with a reasonable agreement with the spectral DNS. Although the polynomial dealiasing approach stabilizes the solution it comes at a large computational cost: the run-time for the high stabilized simulations is increased by a factor of about 30.

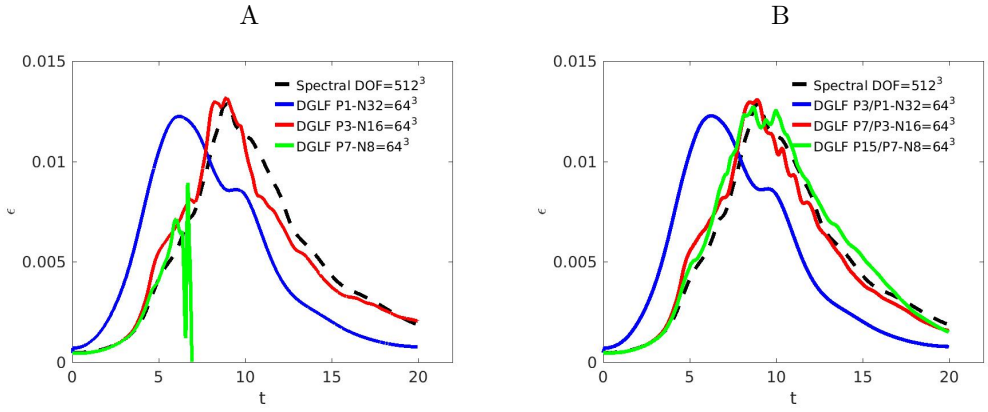

Figure 7. Rate of kinetic energy decay in the Taylor Green Vortex with Re=1600: A: without dealiasing, B: Polynomial dealiasing.

In a recent paper, Gassner et. al have shown[2,3] that kinetic energy preserving flux schemes provide an efficient means of stabilizing under-resolved DG simulations. We confirm this finding here by adopting the Pirozzoli kinetic energy preserving flux scheme in the Taylor Green Vortex with Re=1600. Figure 8 shows a comparison of the kinetic energy decay rate obtained using the Pirozzoli kinetic energy preserving flux scheme (left) and the polynomial de-aliasing (right) approach. Both approaches stabilize the high-order simulation but the PI flux scheme does so at a thirty-times lower computational cost. The low order $P = 1$ simulation shows some oscillations early on in the calculated kinetic energy decay rate. The two higher order PI results display slightly larger decay rates than the corresponding filtered DGLF results. This is due to the faster decay of kinetic energy (recall that $\varepsilon - \frac{dK}{dt}$) in the PI simulations than in the filtered DGLF simulations as shown in figure 9. As observed in the well resolved case above, this finding is somewhat surprising since the Split-Form Pirozzoli method is designed to conserve kinetic energy under convection in the inviscid limit and thus we expected overall less dissipative results.

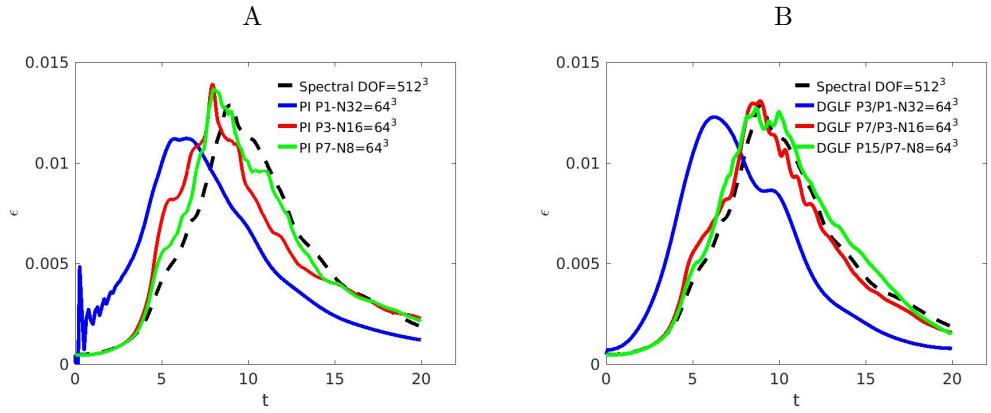

Figure 8. Kinetic energy in the Taylor Green Vortex with Re=1600: A: Split Form Pirozzoli, B: Polynomial dealiasing.

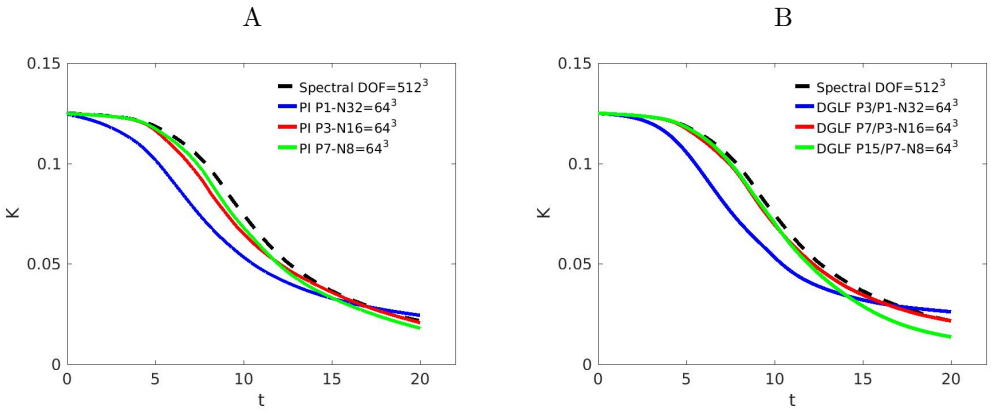

Figure 9. Kinetic energy in the Taylor Green Vortex with Re=1600: A: Split Form Pirozzoli, B: Polynomial dealiasing.

A comparison of the resolved dissipation rate ε_1 predicted by the two approaches is shown in figure 10. The PI results show smaller resolved dissipation rate values than the filtered DGLF results confirming the findings for the kinetic energy decay.

To investigate the question of the increased dissipation in the PI results further, we have performed simulations of the inviscid TG with both PI and filtered DGLF approaches. Figure 11-(A) shows a comparison

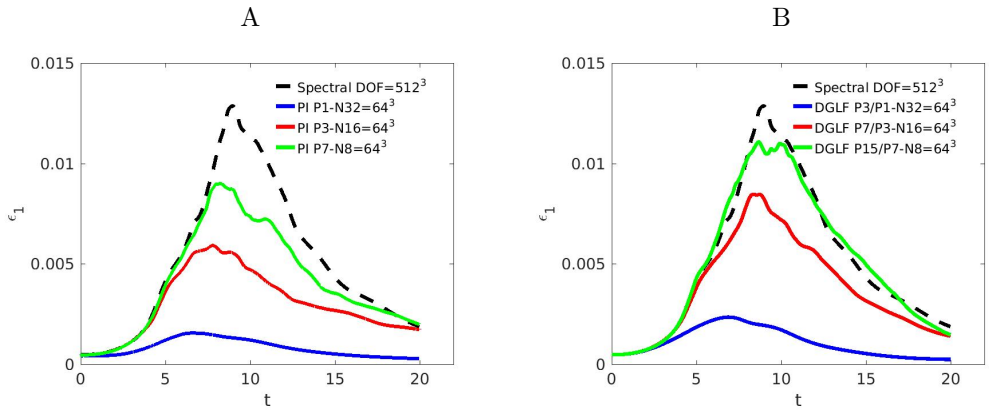

Figure 10. Kinetic energy in the Taylor Green Vortex with Re=1600: A: Split Form Pirozzoli, B: Polynomial dealiasing.

between the filtered DGLF ($P = 7$ filtered to $P = 3$) with $N = 16$, the PI approach with $P3$, $N = 16$ and with $P = 2$, $N = 16$. The figure clearly shows that the PI method indeed very nearly conserves the kinetic energy in the inviscid case. It should be noted that only the lower order $P = 3$ cases could be run to completion, the higher order simulations crashed typically around $t = 5$. In the PI simulation with $P3$ the kinetic energy is not perfectly conserved due to the pressure work ε_3 as was also observed by Gassner et. al.[2] The dissipation of kinetic energy due to ε_3 is shown in (B) and the PI result with $P3$ shows very large values whereas the $P2$ simulation shows negligible values and the filtered DGLF result displays small negative values. It turns out that for the PI method ε_3 is much lower for even polynomial orders than for odd ones.

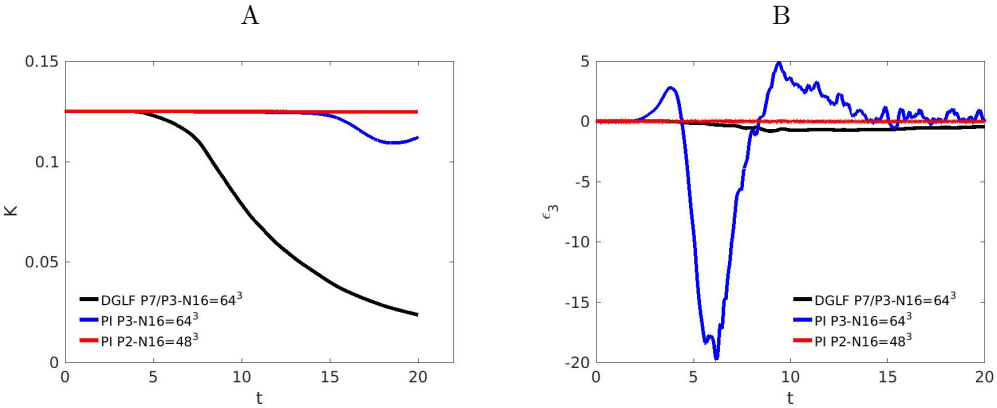

Figure 11. Kinetic energy (A) and dissipation due to pressure work ε_3 (B) in the inviscid Taylor Green Vortex flow.

This is demonstrated in figure 11 where ε_3 is shown for the Re=1600 case obtained from the Split-Form Priozzoli flux approach with even polynomial orders (A) and odd polynomial orders (B) keeping the DOF's approximately constant. The pressure dilation work is about 100 times smaller with even polynomial orders. A comparison of the kinetic energy decay (not shown) reveals no significant differences though. For the remaining of the paper, we will thus consider mostly even polynomial order.

At this point it can only be speculated that the SIP implementation of the viscous terms could cause the slightly increased numerical dissipation observed in PI method. We can indirectly confirm this speculation by considering two additional versions of the Split-Form PI method: the PI-Roe method adds the dissipative part of the Roe flux[18] to the kinetic energy conserving PI flux and the PI-L2Roe adds the dissipative part of a low-dissipation Roe solver.[19] Similar combinations have been considered in reference.[3] It is expected that

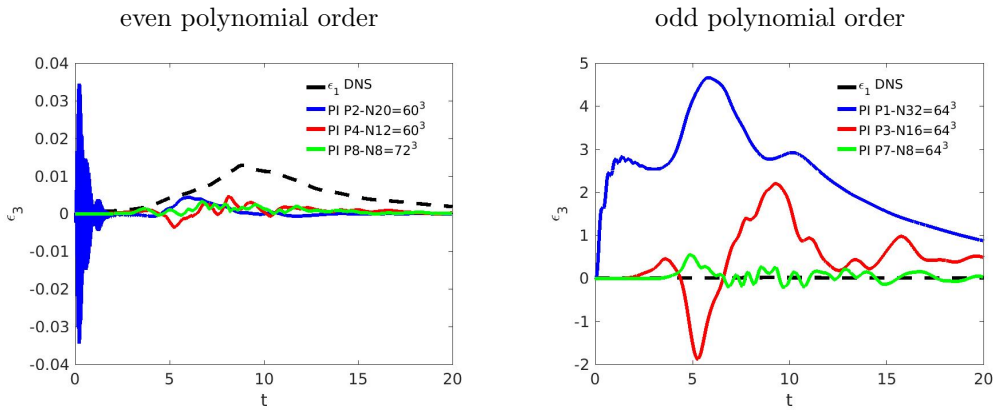

Figure 12. Dissipation due to pressure work ε_3 in the Re=1600 Taylor Green Vortex flow: even polynomial order (left), odd polynomial order (right).

the PI-Roe method is the most dissipative method leading to the largest total kinetic energy decay rate ε and the smallest resolved viscous dissipation rate ε_1. Figure 13 shows a comparison of the dissipation rates obtained with the three methods for a case with $N = 8$, $P = 8$, $DOF = 72^3$. What can be seen is that at early times the total dissipation rate is actually smallest for the PI-Roe method (green line) and the resolved dissipation is largest contrary to what is expected. It can only be speculated that for the PI and PI-L2Roe methods with much smaller convective flux dissipation the viscous flux implemented by SIP is larger so that overall a stronger numeircal dissipation is observed.

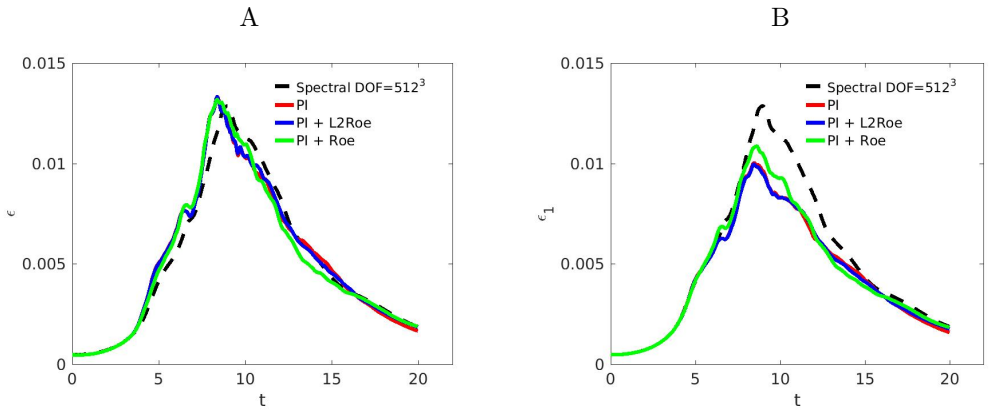

Figure 13. Total dissipation rate (A) and resolved viscous dissipation for the Re=1600 case obtained with the PI, PI-L2Roe, and PI-Roe methods.

C. SGS model results

The SGS models are tested for the Split-Form Pirozzoli flux approach in the Re=1600 TG case with a resolution of $N = 8$, $P = 8$, $DOF = 72^3$. Figure 14 shows a comparison of the no-SGS case, the Smagorinsky model, and the DHM. The constant Smagorinsky model adds dissipation even at the early laminar stages and causes overall a significantly faster decay of kinetic energy. The DHM only adds a small amount of dissipation during after the flow has become fully turbulent. This feature is expected from the dynamic model and can be confirmed here.

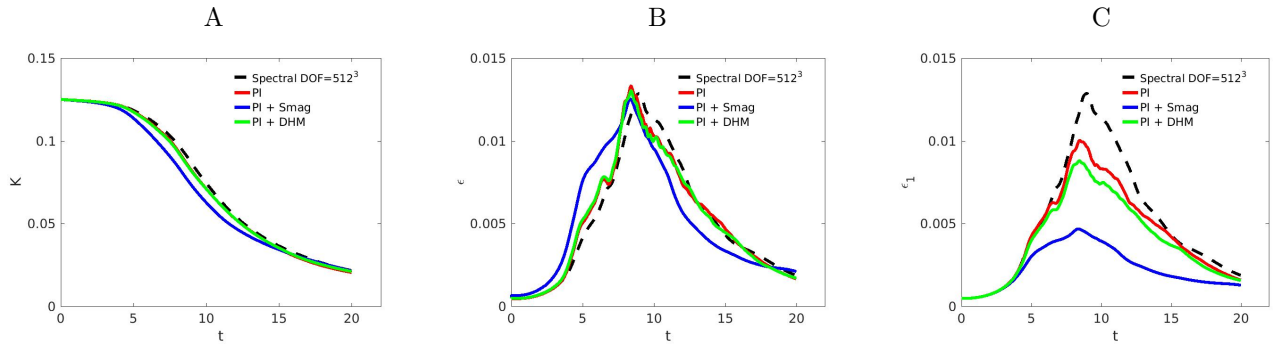

Figure 14. Kinetic energy (A), total dissipation rate (B) and resolved viscous dissipation rate in the Re=1600 TG flow using SGS models.

VI. Summary and Conclusions

The main objective of this work is to investigate the feasibility of using low dissipation kinetic energy preserving split-form DG flux schemes in conjunction with dynamic SGS models for high-order LES. The Taylor Green vortex flow at Reynolds number $Re = 1600$ is considered. We validate the solver using the conventional DG with Lax-Friedrich flux and the new kinetic energy preserving split-form Pirozzoli (PI) method through simulations of a well resolved case by comparison with results obtained from a pseudo-spectral solver. We found that both methods provide very similar results but the PI method actually showed a somewhat larger numerical dissipation. For under-resolved simulations such as LES, the use of high polynomial orders causes numerical instability due to aliasing. Two methods for de-aliasing have been investigated: polynomial de-aliasing through a modal cut-off filter and using the kinetic energy preserving Pirozzoli flux scheme. The later is computationally considerably cheaper albeit slightly more dissipative. It is speculated that the numerical dissipation observed in with the Split-Form Pirozzoli flux is due to the SIP implementation of the viscous term. Not surprising, using a SGS model at the considered highly under-resolved case adds additional dissipation causing the kinetic energy to decay too fast compared to the DNS. The dynamic model does add much less dissipation confirming the overall suitability for transitional flows.

Acknowledgments

This work was supported in part by ONR Grant N00014-14- 1-0045, by the U.S. Department of Energy, Office of Science, Basic Energy Sciences, under Award DE-SC0012671 and by the National Science Foundation's Division of Mathematics research opportunities (Award No. 1622488). Computer time was provided by the NCAR-Wyoming Supercomputing Center (NWSC) and University of Wyoming Advanced Research Computing Center (ARCC).

References

[1]Kirby Robert M., K. G. E., "De-aliasing on non-uniform grids: algorithms and applications," 2003.

[2]Gassner, G. J., Winters, A. R., and Kopriva, D. A., "Split form nodal discontinuous Galerkin schemes with summation-by-parts property for the compressible Euler equations," *Journal of Computational Physics*, Vol. 327, 2016, pp. 39 – 66.

[3]Flad, D. and Gassner, G., "On the use of kinetic energy preserving DG-schemes for large eddy simulation," *J. Comput. Physics*, Vol. 350, 2017, pp. 782–795.

[4]Garnier, E., Adams, N., and Sagaut, P., *Scientific Computation: Large Eddy Simulation for Compressible Flows*, Springer, 2009.

[5]Heinz, S. and Gopalan, H., "Realizable versus non-realizable dynamic subgrid-scale stress models," *Physics of Fluids*, Vol. 24, 2012.

[6]Wang, D. Z., "1st International Workshop on High-Order CFD Methods," .

[7]Brazell, M. J. and Mavriplis, D. J., "3D mixed element discontinuous Galerkin with shock capturing," San Diego, CA, United states, 2013, p. American Institute of Aeronautics and Astronautics (AIAA).

[8]Lax, P. D., "Weak solutions of nonlinear hyperbolic equations and their numerical computation," *Communications on Pure and Applied Mathematics*, Vol. 7, No. 1, 1954, pp. 159–193.

[9]Shahbazi, K., Mavriplis, D., and Burgess, N., "Multigrid algorithms for high-order discontinuous Galerkin discretizations of the compressible Navier-Stokes equations," *J. Comput. Phys. (USA)*, Vol. 228, No. 21, 2009/11/20, pp. 7917 – 40.

[10]Hartmann, R. and Houston, P., "An optimal order interior penalty discontinuous Galerkin discretization of the compressible Navier-Stokes equations," *J. Comput. Phys. (USA)*, Vol. 227, No. 22, 2008/11/20, pp. 9670 – 85.

[11]Jameson, A., Schmidt, W., and Turkel, E., "Numerical solutions of the Euler equations by finite volume methods using Runge-Kutta time-stepping schemes," 1981.

[12]Kirby, A. C. and Mavriplis, D. J., "An Adaptive Explicit 3D Discontinuous Galerkin Solver for Unsteady Problems," .

[13]Blackburn, H. M. and Schmidt, S., "Spectral element filtering techniques for large-eddy simulation with dynamic estimation," *J. Comput. Phys.*, Vol. 186, 2003, pp. 610–629.

[14]Gassner Gregor J., B. A. D., "On the accuracy of high-order discretizations for underresolved turbulence simulations," 2013.

[15]Diosady Laslo T., M. S. M., "Design of a Variational Multiscale Method for Turbulent Compressible Flows," Aiaa cfd conference, NASA Ames Research Center, San Diego, CA, United states, June 2013.

[16]Pope, S. B., *Turbulent Flows*, Press Syndicate of the University of Cambridge, 2000.

[17]Matthew J. Brazell, Michael Brazell, M. S. and Kirby, A., "Using LES in a Discontinuous Galerkin method with constant and dynamic SGS models," *53rd AIAA Aerospace Sciences Meeting including the New Horizons Forum and Aerospace Exposition*, AIAA 2015-0060.

[18]Roe, P., "Approximate Riemann solvers, parameter vectors, and difference schemes," *J. Comput. Phys. (USA)*, Vol. 43, No. 2, 1981/10/, pp. 357 – 72.

[19]Oßwald, K., Siegmund, A., Birken, P., Hannemann, V., and Meister, A., "L2Roe: a low dissipation version of Roe's approximate Riemann solver for low Mach numbers," *International Journal for Numerical Methods in Fluids*, Vol. 81, No. 2, pp. 71–86.